8TH EUROPEAN CONFERENCE FOR AERONAUTICS AND SPACE SCIENCES (EUCASS)
Conference on "Reusable Systems for Space Access". July 1–4, 2019, Madrid, Spain.

Overview of Flight Guidance, Navigation, and Control for the DLR Reusability Flight Experiment (ReFEx)

René Schwarz[1⋆†], *Daniel Kiehn*[2‡], *Guilherme F. Trigo*[3†], *Bronislovas Razgus*[4†], *Andreas Wenzel*[5†], *David Seelbinder*[6†], *Jan Sommer*[7§], *Stephan Theil*[8†], *Markus Markgraf*[9¶], *Michael Dumke*[10†], *Martín Reigenborn*[11†], *Matias Bestard Körner*[12†], *Marco Solari*[13†], *Benjamin Braun*[14¶], *Dennis Pfau*[15§]

† *German Aerospace Center (DLR), Institute of Space Systems*
Robert-Hooke-Str. 7, DE–28359 Bremen, Germany

‡ *German Aerospace Center (DLR), Institute of Flight Systems*
Lilienthalplatz 7, DE–38108 Braunschweig, Germany

§ *German Aerospace Center (DLR), Simulation and Software Technology*
Lilienthalplatz 7, DE–38108 Braunschweig, Germany

¶ *German Aerospace Center (DLR), Space Operations and Astronaut Training*
Oberpfaffenhofen, DE–82234 Weßling, Germany

⋆ Corresponding author

Abstract

This paper gives an overview of the proposed GNC architecture for DLR's Reusability Flight Experiment (ReFEx), which is split into two main subsystems: The Guidance and Control (G&C) subsystem, which determines the desired trajectory from the current flight state to a designated target and issues the necessary commands to the actuators (canards and rudder, as well as a reaction control system for flight phases outside the atmosphere) by calculating the necessary forces and torques based on the required changes of velocity and attitude for following this trajectory; the Hybrid Navigation System (HNS), which is responsible for estimating position, velocity, attitude, angular rates, and other parameters of the flight state. It does so by real-time fusion of measurements of inertial sensors (accelerometers and gyroscopes) with the measurements of GNSS receivers, Sun sensors, laser and radar altimeters. The requirements and boundary conditions set by the mission, the current design baseline for both subsystems, the stability analyses for flight control, the basic guidance strategy chosen as well as the navigation performance assessment through covariance analysis are described and discussed.

1. Introduction

The German Aerospace Center (DLR) is studying future Reusable Launch Vehicles (RLV) with horizontal landing capability. For this purpose, DLR is developing the Reusability Flight Experiment (ReFEx), which is a sub-scale demonstrator representing a winged first stage of an RLV. It has a mass of around 400 kg and is approximately 2.7 m in length with wings spanning about 1.1 m. The mission shall enable the development of key technologies necessary for future RLV applications, culminating in their demonstration with a controlled autonomous return flight in a representative scenario.

In order to bring such space systems back to Earth, determining and actively controlling the flight state, i. e., position and attitude, is essential. These capabilities are usually provided by Guidance, Navigation and Control (GNC)

Revised paper as of July 1, 2019
[1]E-Mail: rene.schwarz@dlr.de, ORCID: 0000-0002-8255-9451
[2]E-Mail: daniel.kiehn@dlr.de, ORCID: 0000-0001-7383-0740
[3]E-Mail: guilherme.trigo@dlr.de, ORCID: 0000-0001-8173-9592
[4]E-Mail: bronislovas.razgus@dlr.de
[5]E-Mail: andreas.wenzel@dlr.de, ORCID: 0000-0002-4370-1291
[6]E-Mail: david.seelbinder@dlr.de, ORCID: 0000-0003-4080-3169
[7]E-Mail: jan.sommer@dlr.de
[8]E-Mail: stephan.theil@dlr.de, ORCID: 0000-0002-5346-8091
[9]E-Mail: markus.markgraf@dlr.de
[10]E-Mail: michael.dumke@dlr.de, ORCID: 0000-0002-5587-7884
[11]E-Mail: martin.reigenborn@dlr.de
[12]E-Mail: matias.koerner@dlr.de
[13]E-Mail: marco.solari@dlr.de
[14]E-Mail: benjamin.braun@dlr.de, ORCID: 0000-0002-0193-6607
[15]E-Mail: dennis.pfau@dlr.de

systems implemented aboard the spacecraft. This paper gives an overview of the proposed GNC architecture for ReFEx, which is split into two main subsystems: The Guidance and Control (G&C) subsystem, which determines the desired trajectory from the current flight state to a designated target and issues the necessary commands to the actuators (canards and rudder, as well as a reaction control system for flight phases outside the atmosphere) by calculating the necessary forces and torques based on the required changes of velocity and attitude for following this trajectory; the Hybrid Navigation System (HNS), which is responsible for estimating position, velocity, attitude, angular rates, and other parameters of the flight state. It does so by real-time fusion of measurements of inertial sensors (accelerometers and gyroscopes) with the measurements of Global Navigation Satellite System (GNSS) receivers, Sun sensors, and radar altimeters. The requirements and boundary conditions set by the mission, the current design baseline for both subsystems, the stability analyses for flight control, the basic guidance strategy chosen as well as the navigation performance assessment through covariance analysis are here described and discussed.

2. Mission and Vehicle

2.1 Mission Description

The main goal of the project is the demonstration of an autonomous re-entry flight of a winged vehicle from hypersonic velocity down to subsonic range. One of the main challenges is the vehicle design that enables a static as well as a dynamic stability of the vehicle in all these flight regimes. This imposes demanding requirements to the vehicle's aerodynamic design as well as the GNC subsystems. Especially the transonic region is challenging, since the position of the aerodynamic center of pressure will rapidly change. The development and demonstration of the corresponding GNC technologies is therefore a central part of the project.

ReFEx shall be launched by a Brazilian solid propellant two-stage VSB-30 rocket from the Royal Australian Air Force (RAAF) Woomera Range Complex, Australia. Following a guided rail travel, the launch vehicle builds up a roll rate aiming to reduce dispersion at payload separation and stage impact. First, the vehicle is unguided and passively stabilized by sets of four fins on each stage. To fulfill the flight stability requirement without major modifications on the launch vehicle, the effective aerodynamic surfaces of the ReFEx payload have to be reduced, which is realized by a foldable wing design and a 0.64 m diameter hammerhead fairing covering the tail section of the ReFEx experiment during atmospheric ascent. In the exoatmospheric flight phase after burn-out of the second stage, a yo-yo system is activated for despin and subsequently the stage is separated from the ReFEx payload.

After separation, ReFEx shall perform a re-entry similar to that of full-scale winged reusable stages. An RLV re-entry corridor was derived based on former research on the Liquid Fly-Back Booster (LFBB) [1] and other winged RLV concepts (e. g., Evolved European Reusable Space Transport (EVEREST) [2]). The mission goal of ReFEx is to achieve a re-entry trajectory in or close to this RLV corridor.

Thus after despin, the vehicle is prepared for the atmospheric entry phase in which the vehicle is controlled by aerodynamic control surfaces (canards and rudder). In the first phase, ReFEx will fly in "belly-up" configuration with the fin pointing down. At a velocity of 2 Ma, a 180 deg roll is performed and the atmospheric flight is continued with the fin pointing up. Finally, ReFEx will pass the transsonic regime and will continue on a glide path down to the ground. A sequence of the mission events is shown in Figure 1. More detailed information about the mission can be found in [3].

2.2 Vehicle Layout

Since the GNC is solely used for the return flight, only the re-entry configuration used during this phase is described. Figure 2 shows the re-entry configuration of ReFEx. It has a length of 2.7 m, a wingspan of 1.1 m, and a total mass of about 400 kg. The Reaction Control System (RCS) for controlling the vehicle's attitude during exoatmospheric phase is located in the aft section. During the atmospheric flight phase, the two canards are mainly used for roll and pitch control, and the rudder mainly for yaw control.

A more detailed description of the vehicle design and all subsystems can be found in [3].

3. Architectural Design of the GNC System

In order to bring space systems like RLVs, shuttles, or microgravity research platforms back to Earth, determining and actively controlling the flight state (for example position and attitude, among others) is essential. These capabilities are usually provided by GNC systems implemented aboard the spacecraft, which fulfill three fundamental functions: The *navigation function* is responsible for estimating position, velocity, attitude, angular velocity, and other parameters of the flight state. The *guidance function* determines the desired path of travel (reference trajectory) from the current flight

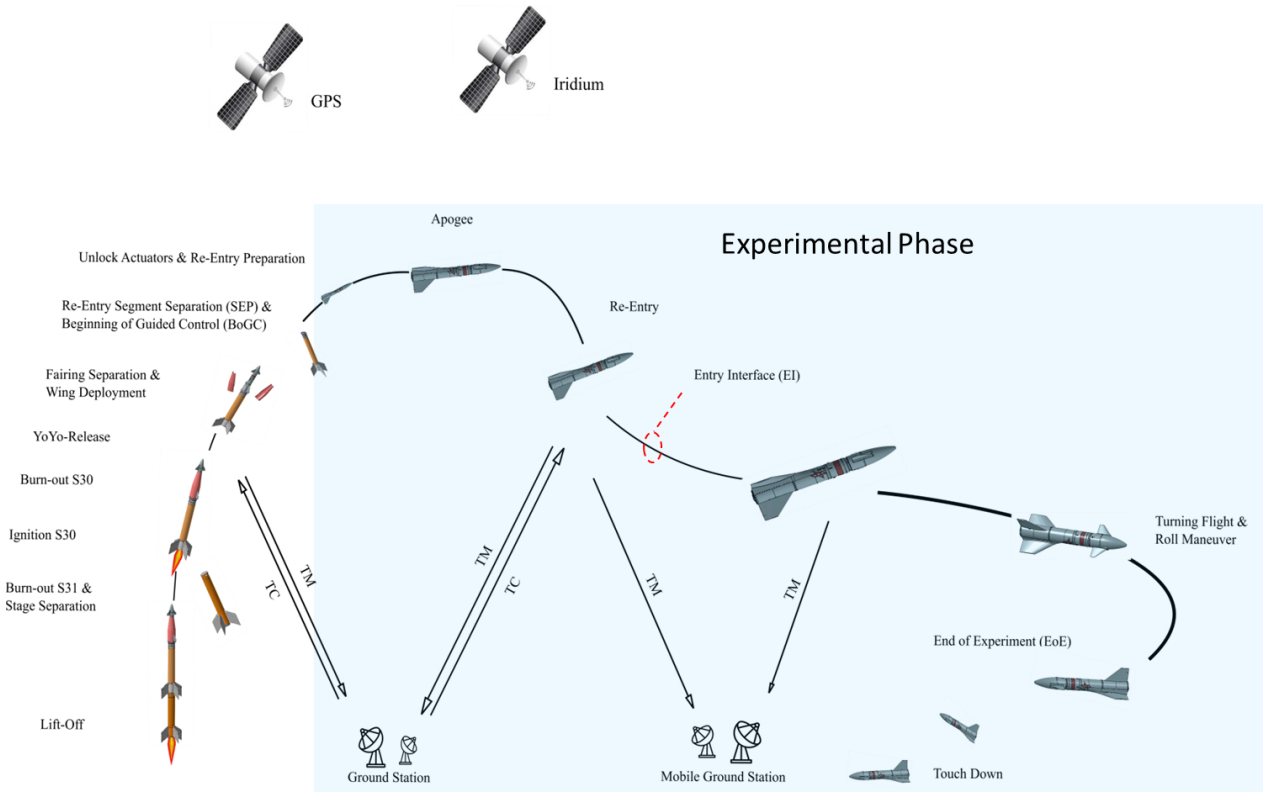

Figure 1: Overview of the ReFEx mission sequence.

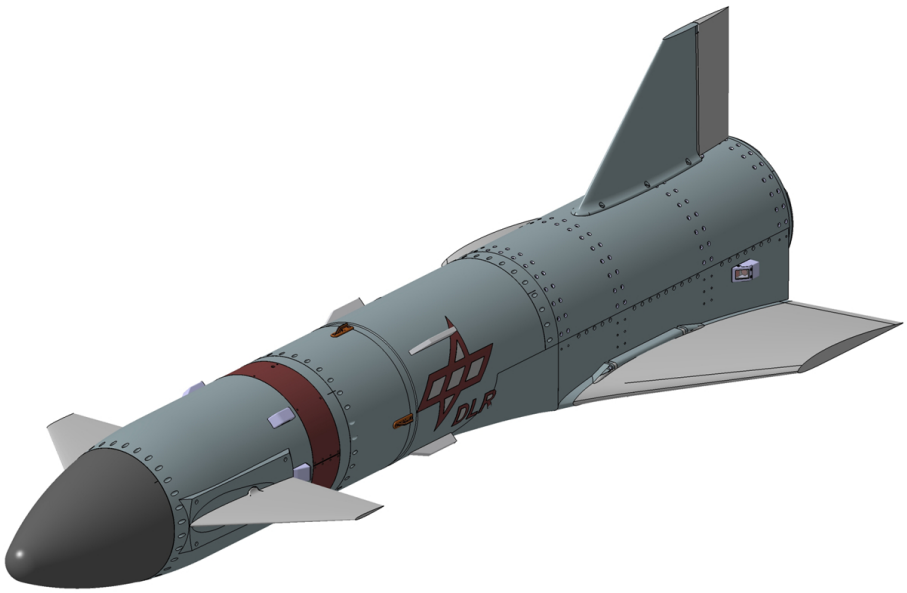

Figure 2: Configuration of the ReFEx payload during re-entry.

state to a designated target by calculating the necessary changes of velocity, attitude, and acceleration for following this reference trajectory. Finally, the *control function* generates the necessary forces and torques for achieving the desired changes in movement by issuing appropriate commands to the actuators whilst maintaining the flight stability and taking the operational capabilities of each individual actuator into account.

GNC systems can be implemented in very different forms, beginning with highly integrated systems combined together with all other functions of a spacecraft on a centralized On-Board Computer (OBC) up to distributed systems with standalone elements for several functions. A highly integrated approach allows for optimizing mass, volume, and energy budgets, but usually requires a complete custom development for a particular mission, which often cannot be simply reused. On the other end, distributed systems with standalone elements allow for a certain partitioning of functions and mostly independent development. This way, the development and verification can be focussed on the particular function more easily, with clear and defined interfaces to other functions. It also allows for a certain degree of modularity and exchangeability between different missions. It has been chosen to develop a distributed GNC system for ReFEx for the aforementioned reasons. A schematic of the simplified functional ReFEx GNC architecture is provided with Figure 3.

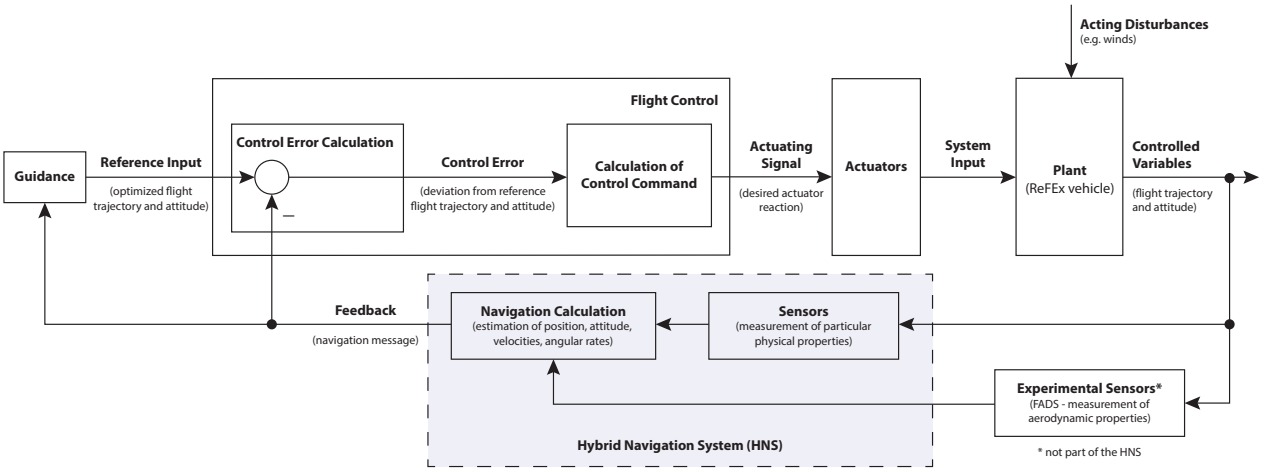

Figure 3: Simplified functional architecture of the GNC system to be developed for ReFEx.

The driving GNC performance goal is the minimization of the dispersion with respect to the nominal state at the end of the experimental phase. The GNC system shall operate fully autonomously for the duration of the mission. To this end, a finite state automaton implements an on-board Mission Vehicle Management (MVM) system. Upon satisfaction of predefined trigger conditions, the flight mode changes, which can include a change of the physical vehicle configuration as well as the selection of GNC subroutines. The MVM constantly monitors the vehicle state and — upon violation of a predefined flight safety corridor — issues commands that will force the vehicle to the ground within the boundaries of a designated safety zone.

3.1 Guidance & Control Subsystem

The guidance and control functions will be implemented into a common G&C System for ReFEx, whereas the guidance part is being developed by the Department of Guidance, Navigation and Control Systems at the DLR Institute of Space Systems in Bremen and the control part by the Department of Flight Dynamics and Simulation at the DLR Institute of Flight Systems in Braunschweig. The G&C System is principally formed of an OBC stack with the appropriate connections to the aerodynamic actuators, the RCS, and the HNS. The guidance and control functions are realized as software applications running on this OBC stack. The GNC Base Software, which is identical for both the G&C System and the HNS OBCs, is developed by the On-Board Software Systems Group of the Department of Software for Space Systems and Interactive Visualization at DLR's Facility for Simulation and Software Technology in Braunschweig.

3.1.1 On-Board Computer

The G&C system consists of one OBC stack together with the corresponding software. The OBC stack is composed of three stackable PC/104-Express boards similar to the ones used in the HNS Box. The three boards are a processor board, a Controller Area Network (CAN) bus interface extension board, and a power supply board. All boards are enclosed within an ruggedized housing, which is a commercially available option. The housing as well as the processor and

CAN bus interface extension boards are purchased from a commercial vendor, while the power supply board has been developed in-house.

Since the processor board does not provide a CAN bus interface as used for the connection to the aerodynamic actuators and the RCS, a CAN bus interface extension board has been added to the OBC stack. It offers four galvanically isolated CAN bus channels with differential transmit capability to the bus in accordance with the ISO 11898 standard.

In order to generate all required Peripheral Component Interconnect (PCI) and Peripheral Component Interconnect Express (PCIe) bus voltage levels to operate the OBC stack, a power supply board has been developed in-house. The commercially available ones are designed for higher power consumption and, thus, are inefficient when operated in the context of the ReFEx G&C. The power supply board has been developed using standard Commercial Off-the-Shelf (COTS) components and is integrated into an empty mounting frame, which fits to the other stack frames.

3.1.2 Actuators

ReFEx's attitude will be actively controlled from the separation until the landing phase. Initially, this will be under vacuum conditions, later under atmospheric conditions. Two actuator systems will be used to control the attitude of ReFEx during the flight. The first system is a Reaction Control System (RCS) based on pressurized gas, whereas the second system uses aerodynamic airfoils to generate lift forces for attitude control. The second system necessitates a dense enough atmosphere to work, whereas the RCS requires consumables which drives the volume budget, especially for atmospheric flight with high disturbances. Both systems can function simultaneously as set by the GNC control algorithm.

The RCS uses gaseous nitrogen feeding cold gas thrusters and will be used to eliminate the rest spin rate after separation from the second stage of the ReFEx vehicle. During the ballistic phase, the attitude will be controlled with the RCS in roll, pitch, and yaw axes until the incident flow towards the aerodynamic surfaces is sufficient for stabilizing the vehicle. The propellant will come stored from a carbon fiber tank at 300 bar and offer 11.5 N in high-thrust mode and 2.25 N in low-thrust mode. The six cold gas thrusters at the rear side of the vehicle are placed to allow them to be used pairwise for force-free roll control. Pitch and yaw control torques will be accompanied by an undesired force. This cannot be avoided due to the placements of the nozzles into a region shielded from the aerodynamic flow during re-entry.

The aerodynamic actuators will take over control at about 50 km altitude. The three control surfaces, two canards and one rudder, shown in Figure 2 can be controlled separately by a self-developed drive motor assembly. This assembly is first of all designed to the expected torques generated by the airfoils, but the assembly includes a safety mechanism that hinders every motion during the ascent phase that could destabilize the launcher, too. After actively unlocking the mechanism a second safety feature ensures that during power outages each drive motor is turned into an end stop by a spring. This guarantees a ballistic (tumbling) flight of the vehicle in case of mission failure to not leave the reserved airspace by inadvertently flying a stable lifted flight. The canards can be deflected in a symmetrically and asymmetrically fashion to mimic the classical control surface functions of an *elevator* and *ailerons*.

3.2 Hybrid Navigation System (HNS)

The Department of Guidance, Navigation and Control Systems of the DLR Institute of Space Systems in Bremen is developing novel, autonomous Hybrid Navigation Systems (HNS), which are standalone systems meant for integration into distributed GNC systems as described before. They implement the navigation function for missions returning RLVs and other spacecraft back to Earth. The HNS technology is based on the results and experiences with the navigation system experiment aboard the SHarp Edge Flight EXperiment II (SHEFEX II) vehicle and the preliminary design of the navigation system for the SHarp Edge Flight EXperiment III (SHEFEX III) study. It is considered as a demonstration and verification of the capabilities of a highly reliable, compact, tightly coupled, integrated hybrid navigation system. The term *hybrid*, in this context, refers to the combination of high-frequency measurements from inertial sensors (accelerometers and gyroscopes) with measurements of a set of non-inertial sensors (e. g., GNSS receivers, Sun sensors, star trackers, laser altimeters, radar systems, etc.) by methods of data fusion. This method along with mechanisms for establishing a 1-failure tolerance within the system allows for a long-term precise navigation solution and robustness against outages of individual sensors. The exact configuration of the sensor suite is mission specific and is selected based on the needs and boundary conditions of the respective mission profile. A HNS is currently not only being developed for the ReFEx mission, but also for Cooperative Action Leading to Launcher Innovation for Stage Tossback Operation (CALLISTO) project — an international cooperation project between the Centre National d'Etudes Spatiales (CNES), DLR, and the Japan Aerospace Exploration Agency (JAXA), which aims for the development of a flight demonstrator for a Vertical Takeoff, Vertical Landing (VTVL) RLV. Their development is closely linked with each other.

3.2.1 Fundamental Functions

Derived from the mission and GNC needs, the HNS will implement the following fundamental functions:

1. *Navigation as Part of the GNC Chain*
   Providing an estimation of the vehicle state as feedback to the other elements of the GNC chain, and therefore closing the GNC loop, is the main purpose of the HNS. It does so by providing a high-frequency navigation solution to the G&C computer.

2. *Mission Vehicle Management (MVM)*
   In order to coordinate the operational state of all subsystems, the MVM collects and evaluates information from sensors and — while on ground — manual commands from operators to switch between predefined modes of operation. The information about the current mode of operation is distributed to all subsystems as part of the navigation solution to avoid additional interfaces.

3. *Time Reference/Synchronization*
   The HNS establishes the time reference for the entire ReFEx vehicle and provides two means for time synchronization: For absolute synchronization of time, the navigation message contains a date and time field. A dedicated electrical square wave signal accurately repeating once a second, called a Pulse Per Second (PPS), is generated by the HNS and can be used for phase and frequency synchronization between all clocks aboard the vehicle.

4. *Navigation for Flight Safety Purposes*
   To provide another source of information about the vehicle location for flight safety purposes, an interface for transmitting the raw GNSS receiver messages to ground is implemented. The GNSS receiver technology is flight proven in many DLR missions and, thus, considered as very reliable. The receiver output is independent of the remaining HNS, despite of the powering via the internal Power Distribution Unit (PDU).

5. *Navigation for Correlation of Experimental Data*
   The navigation solution is used to correlate experimental data with navigation information. It is probably provided in a lower frequency than the navigation solution used for G&C to allow transmission over standard serial communication links without hardware flow control.

6. *Navigation for Localization to Support Vehicle Recovery*
   In order to provide the position of the vehicle independent of the ground-based Telemetry (TM) system, an Iridium transmitter and two antennas are included in the HNS. It will periodically send the vehicle position via the Iridium satellite network to a server which is forwarding this information to the HNS Electrical Ground Support Equipment (EGSE).

3.2.2 Baseline Design

The entire HNS architecture is designed as a highly reliable and fault-tolerant system as it is considered as a central element within the GNC loop. Figure 4 provides an overview about the HNS and its components. In terms of sensors, it is equipped with an in-house built Inertial Measurement Unit (IMU) with modified COTS gyroscopes and analog COTS accelerometers, four Sun sensors, two GNSS receivers, one laser altimeter, and one radar altimeter. In addition to that, the HNS uses the Flush Air Data System (FADS) from the set of scientific instrumentation sensors as additional measurement source. The IMU consists of four COTS accelerometers and four modified COTS gyroscopes in a tetra-axial configuration. The HNS also comprises a highly reliable, fault-tolerant on-board computing and data handling architecture with the necessary infrastructure components (e. g., a fully redundant power distribution unit) incorporating a Failure Detection, Isolation, and Recovery (FDIR) scheme. Its key characteristic is an augmented, double modular hot-redundancy scheme of two on-board computer nodes. The main component is the HNS Box, which is a compact, self-contained compartment accommodating the inertial sensors, the GNSS receivers, On-Board Computing and Data Handling (OBCDH) components, the internal PDU, and auxiliary electronics. It is integrated into the ReFEx vehicle in vicinity to its center of mass.

The Sun sensors, GNSS and Iridium antennas as well as the laser and radar altimeters are to be accommodated on the vehicle exterior and are connected to the HNS Box, while the GNSS Low-Noise Amplifier (LNA), band-pass filter, and power divider are to be accommodated within the vehicle close to the GNSS wrap-around antenna. The FADS is used as a measurement source, but it does not belong to the HNS. The HNS has data interfaces to the G&C subsystem, to the Telemetry and Telecommand (TM/TC) subsystem, and to some other subsystems and experiments.

3.2.2.1 Inertial Measurement Unit

The proper functioning of the IMU is vital for the navigation system as the high-rate measurements of angular velocities and linear accelerations, integrated to generate a position, velocity, and attitude solution, ensure the continuity of the navigation output. This continuity is fundamental since possible gaps in the measuring of the high dynamics experienced by the ReFEx vehicle could cause large losses in navigation solution accuracy which in turn could lead to unrecoverable flight states. The IMU is designed as tetra-axial configuration of four modified COTS gyroscopes and four COTS analog accelerometers with an in-house developed Front-End Electronics (FEE). This design allows a partly redundant linear acceleration and angular velocity measurement scheme, thus offering an over-determined measurement system for the three spatial axes. In the event of failure of one sensor, the remaining three sensors will still cover all three spatial axis. All components are mounted onto a self-developed mechanical structure. Since ReFEx will spin with up to 4 Hz around its roll axis, the measurement range of the COTS gyroscopes was extended to cover approx. ±1,500 °/s.

3.2.2.2 GNSS Subsystem

The GNSS subsystem of the HNS is based on the flight-proven Phoenix-HD Global Positioning System (GPS) receiver (Figure 5 (left)) developed at DLR/German Space Operations Center (GSOC) specifically for use in space and high-dynamics projects [4, 5]. The Phoenix-HD offers single-frequency Coarse Acquisition (C/A) code and carrier phase tracking on 12 channels and can be aided with either real-time, or alternatively, a priori trajectory information to safely (re-)acquire GPS signals even at high velocities and accelerations. The receiver is based on a check-card-sized com-

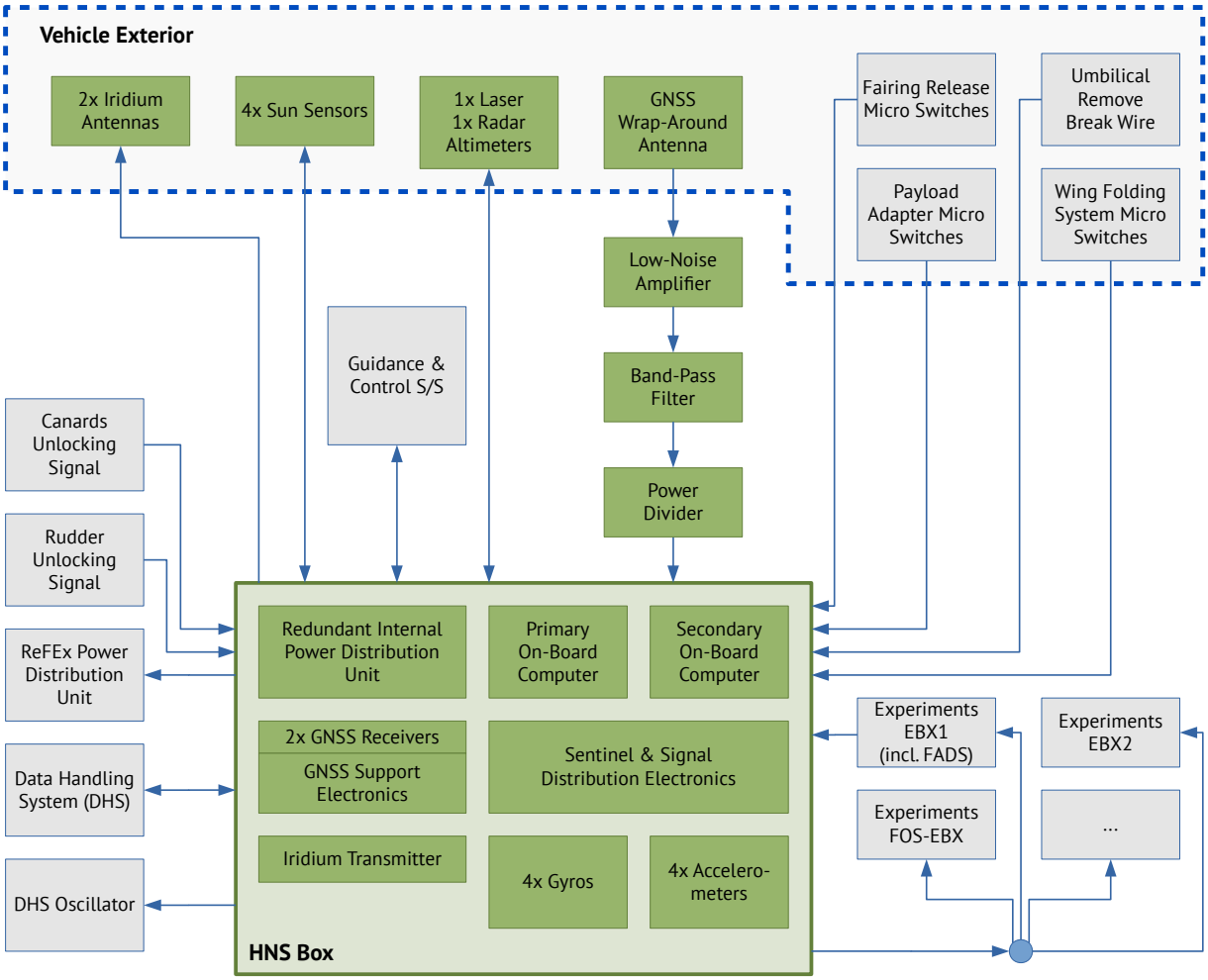

Figure 4: Overview of functional groups and components of the Hybrid Navigation System (HNS) and their locations within and on the ReFEx vehicle. The connections between the components represent the data flow without further distinction between signal types. Green boxes are functional groups and components directly belonging to the HNS.

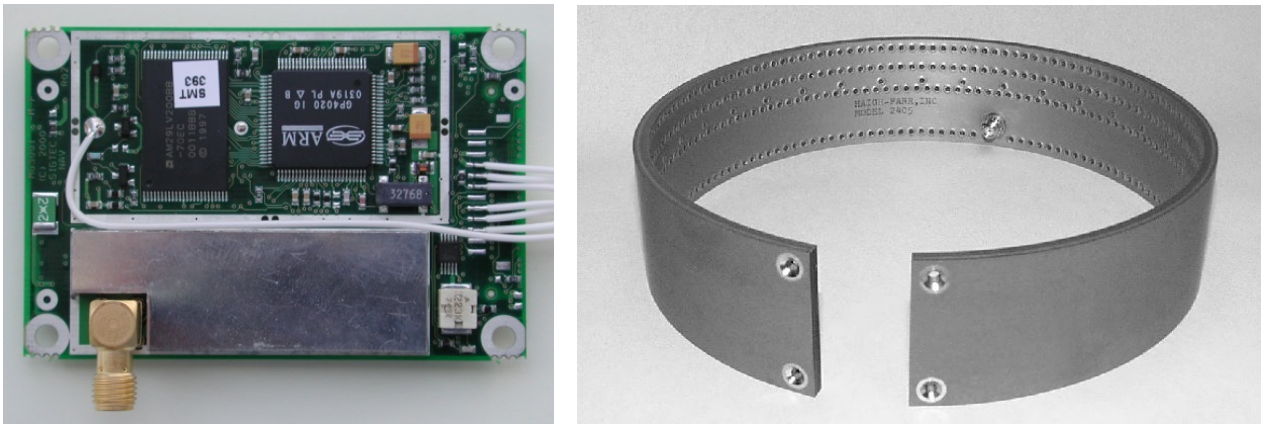

Figure 5: Core components of the GNSS subsystem of ReFEx: Phoenix-HD GPS receiver board (left) and example picture of a GNSS wrap-around antenna for sounding rockets and missiles (right).

mercial hardware platform [6], built around the GP4020 baseband processor of Zarlink, combined with a firmware developed by the GNSS Technology and Navigation Group at DLR's GSOC for space applications. The receiver was successfully employed in several dozens of national and international sounding rocket, launcher, and Low-Earth Orbit (LEO) satellite projects over the last decade. In the ReFEx project, the receivers will provide position and velocity fixes as well as GPS raw data (pseudoranges and range rates) to the navigation computer for fusion with data from other position and attitude sensors. Moreover, the GNSS subsystem will provide timing information in terms of a PPS signal and corresponding time messages to the vehicle.

A redundant pair of Phoenix-HD receivers will be accommodated in a common enclosure along with an electrical interface board specifically designed and build for this mission. The design of this so-called GPS main electronic unit has been chosen such that in future projects utilizing the HNS modifications, e. g., of the employed navigation receivers or the redundancy concept, can be applied without the need to also change the electrical or mechanical interface of the main electronic unit.

For the reception of GPS signals during the flight, a single GNSS wrap-around antenna (Figure 5 (right)) will be used. The main advantages of this type of device are the almost omnidirectional receiving pattern as well as the spin-insensitivity of the antenna. It will be flush-mounted into the cylindrical part of the structure of the ReFEx re-entry vehicle in between the nose cone section and the wing section but outside of the fairing. The choice of a wrap-around antenna and the above mounting position allows for a proper signal reception, and thus availability of a valid GPS navigation solution, throughout all flight phases from lift-off to landing. In order the make the antenna resistant to the high temperatures expected during launch and re-entry, an ablative heat shield is added to the antenna by the manufacturer.

Figure 6 provides a structural overview of the complete GNSS subsystem architecture. In between the above already addressed wrap-around antenna and main electronic unit, a dedicated GPS LNA, also developed at DLR for space missions, and a COTS passive power divider will be inserted to complete the GNSS subsystem of the HNS for ReFEx. An optional match-box-sized GPS L1 band-pass filter may further be added in between the LNA and power divider in case GPS interferences are detected during the system-level tests to be conducted once all components and subsystems are available for such testing.

3.2.2.3 Sun Sensors

Digital two-axis COTS Sun sensors are utilized within the HNS sensor suite to aid the attitude estimation process, especially to reduce the estimation errors after the yo-yo despin maneuver. Four Sun sensors are equidistantly placed around the circumference of the longitudinal body axis of the vehicle. Each Sun sensor has a Field of View (FoV) of 120 deg in each axis and measures the Sun position with an accuracy better than 0.3° (3σ). The sensors are directly connected via dedicated RS-422 serial interfaces to the HNS Box, from which they are also powered.

A preliminary illumination analysis has been carried out along with an update of the HNS performance assessment already presented in [7]. The results are explained in Section 6.

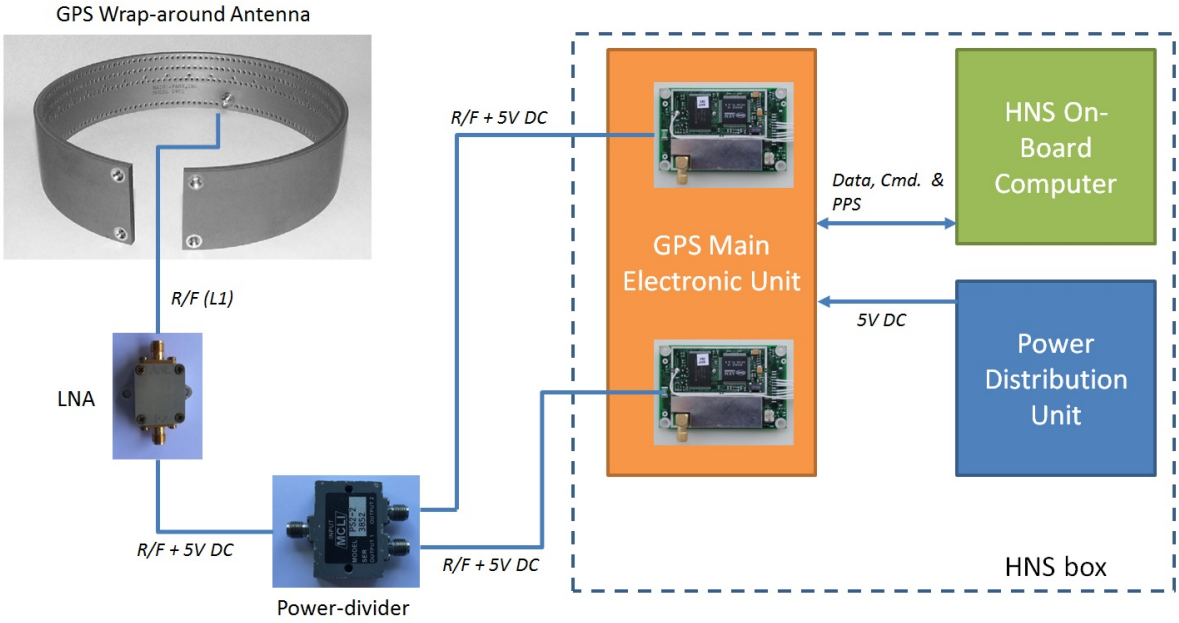

Figure 6: Structural diagram of the GNSS subsystem architecture for ReFEx.

3.2.2.4 Laser and Radar Altimeters

During the final flight phase, execution of a flare maneuver prior to touchdown is planned in order to reduce the remaing energy — most notably the vertical speed component — and therefore decreasing the damage to the vehicle. The good knowledge of the altitude over ground is required to estimate the point when the maneuver will be initiated. To avoid the need of a terrain model to back-calculate the altitude over ground from the navigation solution, a dedicated sensor suite will be implemented.

The selected sensor types are laser and radar altimeters. Both sensor types are COTS available for aeronautical or drone applications, offering heritage and reliability. Furthermore both type of sensors are available in small packages, easing an implementation in the ReFEx vehicle. The selected laser altimeter has a range of over 1,500 m, while the true altitude over ground may be back-calculated using the known vehicle attitude. The selected radar altimeter offers an altitude solution starting at 100 m over ground and with an update rate of up to 800 Hz. The sensors will be integrated facing downwards to the ground during the final approach. Protective materials will ensure that the sensors take no harm during the hypersonic and supersonic phase since both sensors will need a cut-out through the metallic outer shell of the vehicle.

3.2.2.5 On-Board Computing & Data Handling

In order to enable the HNS to perform all its functions, a highly reliable, fault-tolerant OBCDH architecture with the necessary infrastructure components (e. g., a fully redundant PDU) incorporating a FDIR scheme is being developed. Its key characteristic is an augmented, double modular hot-redundancy scheme of two OBC nodes. The OBCs are stackable COTS single-board computers with Intel Atom Quad-Core Central Processing Units (CPU) in the standardized PC/104-Express format. The OBC stacks are extended with custom interface extension boards based on a Xilinx Spartan-6 Field-Programmable Gate Array (FPGA), providing a large amount of RS-422/485 serial communication links, General-Purpose Input/Outputs (GPIO), and Ethernet ports. Each OBC stack will be supplied by one in-house developed power supply board.

The OBCs are operated in a hot redundancy scheme, i. e., each OBC receives the data of all components and performs all calculations with the same on-board software. However, only one OBC is the *currently active OBC* whose outputs (commands) will be routed to the respective components within the HNS or to the outside world (i. e., the navigation solution, telemetry, etc.). All outputs of the other OBC (referred to as *standby OBC*) are suppressed by an electronic circuitry. In case of failure of the currently active OBC, the system can switch the roles of both OBCs, so that the output of the previous standby OBC will be routed. After switching the roles, the failing OBC will be power cycled and tested. There are various failure detection mechanisms in place in order to ensure a proper and timely role switch in case of failures.

The OBCDH systems closely interact with the PDU, which is controlled by the OBCs and delivers valuable monitoring data back. This way, it is also possible for the OBC to detect power anomalies and switch certain devices on or off to safeguard or recover the system operation. The PDU also plays a vital role for initialization of the HNS as it ensures a sequential and proper activation of all components, especially the OBCs.

3.2.2.6 Power Distribution

The PDU is a 1-fault-tolerant power supply developed [8, 9, 10] for the ReFEx HNS and is located within the HNS Box. Its main task is to monitor and control the supplied power for all devices within the HNS system boundary. It includes redundancy of all its critical components and a PDU Monitor (PDU-M) that monitors currents, voltages, and temperatures. All these measurements are then transmitted to the PDU Controller (PDU-C) which uses these measured variables in its algorithms to define the switch status [11]. Since the HNS electronic devices are sensitive to power supply voltage variations, overvoltage protection had been also included.

The PDU has, among others, Electromagnetic Interference (EMI) filters, resettable electronic fuses, electronic switches, Direct Current-to-Direct Current (DC/DC) converters and O-Ring (OR) diodes. EMI filters are used to prevent the high-frequency currents generated in DC/DC converters to flow back to the vehicle power supply. Resettable fuses provide overcurrent protection for each switch. If one electronic fuse trips, it can be reset by switching the corresponding switch off and on once the switch temperature is back within the limits. Each electronic switch controls the applied power to each load. Primary switches control the input power for each DC/DC converter, while secondary switches control the power to the HNS devices. DC/DC converters are used to lower the bus voltage level to the desired one. Finally, OR diodes are used to isolate each DC/DC converter output [12]. Figure 7 shows the redundant power channel diagram configuration.

In case one switch fails, the PDU redundant concept allows the output device to receive power from its redundant power supply line. Besides that, if the PDU-C fails, the fail-safe mode procedure will start. Using a watchdog, the PDU can detect errors in the PDU-C if no or wrong stimuli signals are generated. When the fail-safe mode starts, all power channels are enabled and all HNS devices are powered. Since the fail-safe mode cannot be deactivated, the switch control is lost, but the overall system operation is not affected because all devices were switched on [13].

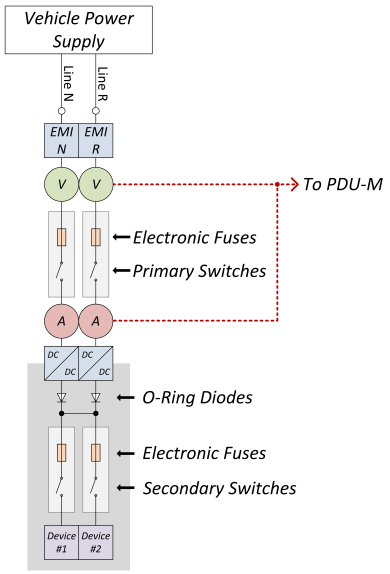

Figure 7: PDU redundant power channel diagram.

3.3 Base Software

The on-board software of the G&C and HNS OBCs needs to fulfill a number of complex tasks in a timely fashion while being distributed among multiple OBCs. This includes beside the GNC functionality itself, the distribution of the on-board time to other subsystems, the management of the overall mission state, and the generation of telemetry data, both live data for immediate downlink as well as high-rate data for post-flight analysis. The base software includes most notably the operating system including experiment-specific drivers, the hardware abstraction, the execution runtime for the GNC algorithms and the background services for communication with other subsystems, e. g., the distribution of the global time reference.

3.3.1 Operating System

All of the above mentioned services need eventually be supported by the underlying base software and in turn drive its design decisions. Firstly, the state estimation of the HNS as well as the computation of the control solution in the Guidance & Control Computer (GCC) need to be executed in precise time windows. Therefore, the base software support for execution in a real-time context is a key requirement. The algorithms for the GNC subsystems are expected to be complex with regard to the computational performance requirements. That means, the base software needs to provide enough computational reserves by fully supporting the multicore CPUs of all OBCs and the distribution of software tasks among those cores. Naturally, the base software needs to implement drivers for all low-level interfaces which are used for communication with connected sensors and actuators or other remote terminals.

Based on those basic requirements, Real-Time Executive for Multiprocessor Systems (RTEMS) [14] was selected as operating system. It is an open source real-time operating system which supports a large set of different hardware architectures and with a long heritage in space-related applications. In its most recent version, it provides a real-time executive and real-time schedulers for Symmetric Multiprocessing (SMP) on multicore systems. The programming interface even supports multiple scheduling groups and thread pinning for distributing the workload among the processor cores with certain constraints [15]. However, the RTEMS port for x86-based hardware platforms did not have a functional implementation of the SMP scheduling system. Therefore, as a first development step, the code base has been extended to support SMP for the x86-based OBCs of ReFEx. The open source nature of RTEMS also allows to integrate drivers for the custom-made interface board of the HNS OBC (see Section 3.2.2.5) which are the basis for the communication with sensors, actuators, and other subsystems.

3.3.2 Middleware

The planned development cycle for the ReFEx on-board software is comparably short and available development resources are limited. With all OBCs being based on the x86 architecture, the goal is to share as much code as possible among them and reuse existing DLR software technologies where suitable. That means, all OBCs will use the same operating system but with differing driver implementations as their interface devices are not completely the same. The middleware layer is responsible for hardware abstraction and providing an execution runtime for the application layer software, e. g., the control algorithms. The hardware abstraction is done in two steps. First, a common Application Programming Interface (API) for the actual interface devices is used in order to separate the device time, e. g., serial or CAN bus connection from the low-level operating system driver. The second layer then uses this common API to provide access to connected devices, i. e., the sensors and actuators, to the application layer. For the hardware abstraction layer, DLR's Open modUlar sofTware PlatfOrm for SpacecrafT (OUTPOST) library [16] will be used and extended with new interface and device drivers as needed.

The execution runtime for the GNC algorithms will be provided by DLR's own Tasking Framework [17] which has been successfully used in attitude control systems in previous missions, e. g., the Compact Satellite mission "Euglena and Combined Regenerative Organic-Food Production in Space (Eu:CROPIS)" [18]. The algorithms themselves are partitioned into smaller stateless tasks which exchange data via one or multiple channels. The channels hold the input data or control the timed activation of the tasks' inputs. When all necessary inputs for a task are activated through available data or a timed event, a task is scheduled as soon as possible.

3.3.3 Development Methodology

The overall software development is carried out by a distributed team of developers and engineers, where most of them do not have direct access to actual flight hardware or a Hardware-in-the-Loop (HiL) setup for most of the time. Most parts of the middleware, i. e., the OUTPOST library and the Tasking Framework are implemented using a subset of the C++ programming language which encourages strong typing and most notably does not allow the use of dynamic memory allocation during runtime or the use of exceptions. Both libraries also use abstract classes for interface definition extensively, thereby enabling easy setup of test cases with mock classes for hardware devices in order to test higher level functions without flight hardware. They can both be compiled for the RTEMS real-time operating system and for common Linux workstations. This allows to write and execute large parts of the testsuite on common development workstations with a large set of development and analysis tools available and in turn reduce the amount of on-hardware testing significantly during the development phase.

4. Stability Analyses and Flight Control Design

4.1 Stability Analysis and Finding a Suitable Trajectory

The flight dynamics model used for the stability analysis of ReFEx is implemented in MATLAB/Simulink™. It incorporates the nonlinear equations of motion in six Degrees of Freedom (DoF) in a quaternion-based implementation, a World Geodetic System 1984 (WGS84) geodetic model, and the International Standard Atmosphere (ISA) model. Analysis of previous configurations of the ReFEx vehicle revealed severe instabilities in certain flight regimes which made clear that the trajectory that was originally foreseen could not be achieved with the flight control hardware foreseen for the project [19]. In order to find a feasible solution, the configuration was changed as little as possible and a bottom-up approach was used to find a trajectory along which the vehicle is sufficiently stable during the whole flight.

To find a suitable trajectory or flight corridor where ReFEx shows sufficient stability and control authority, a large envelope of discrete points was defined by varying the Mach number, the angle of attack α and the altitude,

resulting in a discrete 3-dimensional array of points. The exact flight condition in each point was obtained by trimming for an equilibrium of rotational accelerations (i. e., $\dot{p} = \dot{q} = \dot{r} = 0$) — note that translational accelerations have to be accepted in the case of ReFEx as there are no engines and no redundant control surfaces. Numerical linearization around a resulting trim point then yields the corresponding system matrix A for this flight condition, and the eigenvalues λ_i of A describe the system dynamics.

Since the hardware to be used in the project was not yet fully known at this stage of the design phase, the acceptable limits for potential instabilities had to be defined by experience. The real part of each characteristic motion (each eigenvalue or pair of eigenvalues) was used to evaluate the stability of the corresponding flight point, utilizing the fact that the time to half amplitude (or double amplitude for unstable motions) t_{HA} relates to the real part of the corresponding eigenvalue via $t_{\mathrm{HA}} = -\ln(2)/\operatorname{Re}(\lambda_{\mathrm{i}})$ [20]. The highest real part of all eigenvalues in a certain flight condition is then considered as the most critical one concerning the stability, regardless of the physical motion behind it. This approach is conservative since some disturbances will be easier to control than others (e. g., the pitch authority is significantly higher than roll authority), but at this stage of the aerodynamic design the same strict criteria shall be used. Based on experience, the maximum admitted real part $\mathrm{Re}_{\mathrm{max}} = \max(\mathrm{Re}(\lambda_i))$ was defined as 0.1 rad/s, i. e., if $\mathrm{Re}_{\mathrm{max}} > 0.1$ rad/s, the flight point is considered insufficiently stable. The longitudinal motion and lateral motion were analyzed separately (which is valid since the nominal flight condition is symmetric, i. e., $\beta = p = q = r = 0$ and either $\phi = 0°$ or $\phi = 180°$), but for the final evaluation only the highest occurrent real part is considered as it represents the least stable motion at this flight point. It is expected that the choice of 0.1 rad/s as the maximum admissible value is overcautious regarding the final performance of the GNC system, but a conservative choice had to be made at this stage of the design process.

The results of the aforementioned analysis are visualized in Figure 8. Flight conditions (combinations of Mach number, angle of attack, and altitude) where a moment equilibrium cannot be achieved are designated as untrimmable (dark gray). If the flight condition is trimmable but the vehicle has insufficient control authority, this point is also undesirable and is marked in light gray. The stability of a flight point is marked in a color only if trimmability exists and control authority is sufficient; the color represents the range of the maximum real part where green represents natural or at least neutral stability, red means insufficient stability, and yellow and orange represent intermediate ranges. Note that a negative angle of attack implies that the airflow hits the vehicle from the top — such a flight point can only be

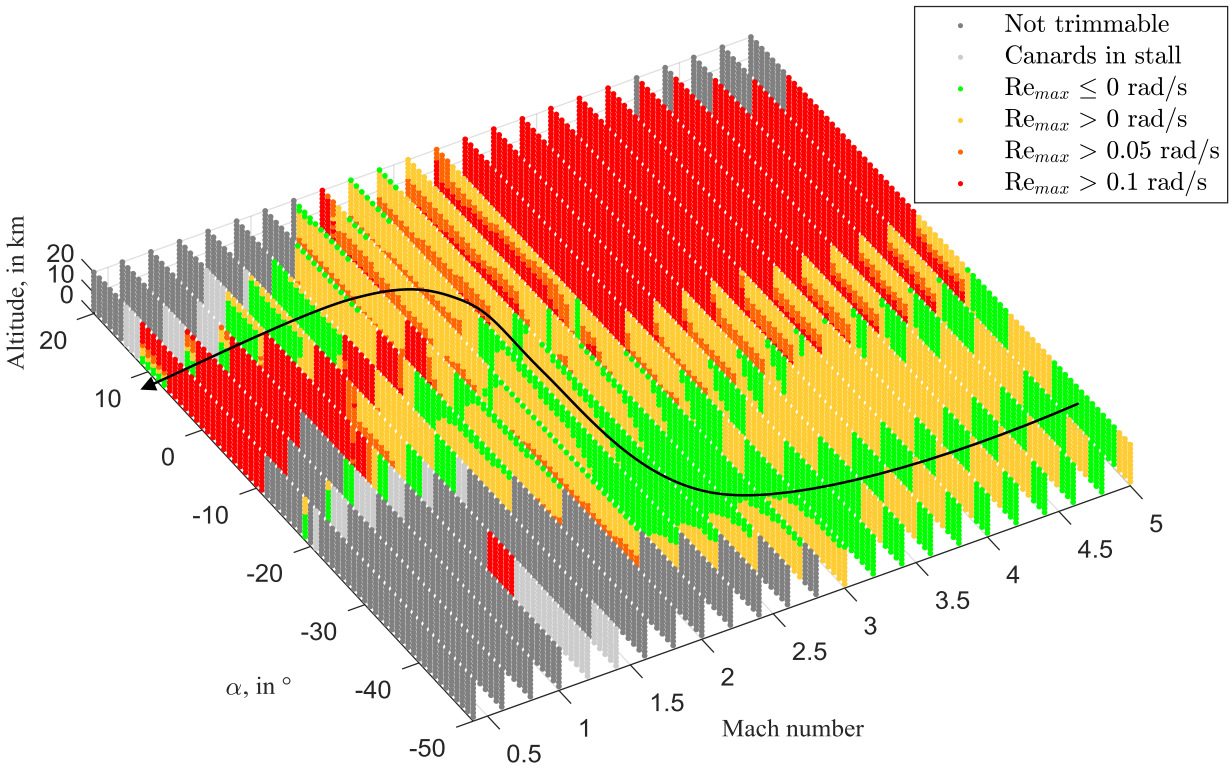

Figure 8: Three-dimensional stability envelope (black: exemplary flight path).

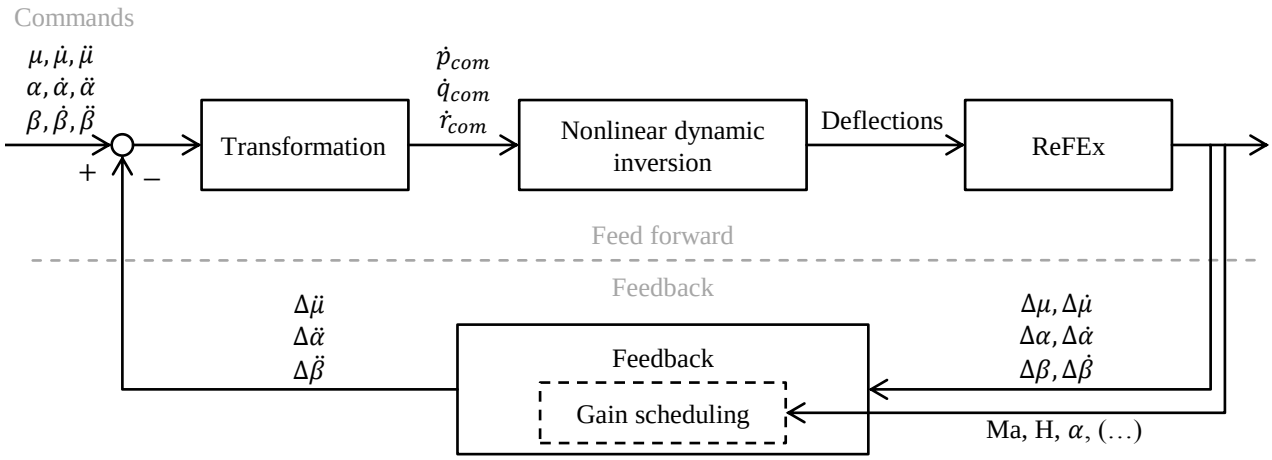

Figure 9: Inner control loop architecture.

meaningful as a nominal flight condition if the vehicle flies upside down. Hence, in Figure 8, a positive angle of attack ($\alpha \geq 0$) corresponds to a belly-down configuration ($\phi = 0°$) and a negative angle of attack ($\alpha < 0°$) corresponds to a belly-up configuration with the fin pointing downwards (i. e., $\phi = 180°$). It is apparent that the vehicle is insufficiently stable in the region of Mach 3 to Mach 5 and angles of attack α higher than approx. $-10°$. The cause for this is that the longitudinal motion is statically unstable here ($C_{m\alpha} > 0$), but also the lateral motion is unstable for higher angles of attack (approx. $\alpha > 10°$) due to the vertical tail being in the wake of the vehicle. As a consequence, the region of higher Mach numbers will have to be flown with the fin pointing downwards. In lower Mach number regimes however, the vehicle is not trimmable in belly-up configuration anymore, causing the need for a roll maneuver to change from belly-up to belly-down configuration. This roll manoeuver could be used to rotate the vehicle, e. g., from $\phi = 180°$ and $\alpha = -20°$ to a belly-down configuration with $\phi = 0°$ and $\alpha = 10°$ at a speed of Mach 2. The flight controller has to coordinate the roll, pitch, and yaw accelerations during this roll manoeuver to ensure that the sideslip angle remains near zero while the bank angle and the angle of attack follow their desired profiles to keep the thermal loads at a minimum (this is often referred to as the velocity vector roll). After the roll manoeuver, ReFEx continues to decelerate in belly-down configuration. Note that the corridor of sufficiently stable angles of attack for Mach < 1 is very narrow, posing high requirements on the GNC system as a whole. Recalling however that the value of 0.1 rad/s defined for $\mathrm{Re}_{\mathrm{max}}$ is expected to be overcautious, the actual flyable Ma/α/altitude corridor is expected to turn out larger than the narrow region in Figure 8.

4.2 Controller Design

The task of the flight controller is to augment the stability of the vehicle and to ensure that it follows the trajectory planned by the guidance system. The primary inputs (commands) from the guidance to the flight control system are the aerodynamic bank angle μ, the angle of attack α and the sideslip angle β, as well as their first and second derivatives to achieve smoothness and continuity. This set of inputs is processed internally in the control software, utilizing the navigation data provided by the HNS, to obtain the corresponding body-fixed rotational rates $(p, q, r)^T$ and accelerations $(\dot{p}, \dot{q}, \dot{r})^T$. Using nonlinear dynamic inversion, the control surface deflections required to achieve the desired accelerations are calculated and commanded to the actuators (feed forward).

The response of the vehicle is measured and deviations from the commanded aerodynamic bank angle, angle of attack and sideslip angle are determined. Using a gain scheduling based on the current flight point (e. g., Mach number, angle of attack, dynamic pressure, etc.) additional $\Delta\ddot{\mu}$, $\Delta\ddot{\alpha}$, and $\Delta\ddot{\beta}$ terms are obtained from the aforementioned deviations and are subtracted from the guidance commands as feedback terms. This combination of feedforward and feedback elements ensures a fast command response and good disturbance rejection. Figure 9 shows an overview of the architecture of the inner control loop.

Time simulations were conducted for preliminary evaluation of the controller design and to validate the implementation of nonlinear dynamic inversion. Since the inner flight controller loop is not yet integrated with the outer guidance loops, the input commands $(\mu_{\mathrm{com}}, \alpha_{\mathrm{com}}, \beta_{\mathrm{com}})^T$ for the simulations were taken from reference trajectories used in the design process of the guidance algorithms. [21] The simulations were performed with realistic actuator models, but assuming perfect (accurate and undelayed) measurements of the vehicle's position, attitude, etc. The assumption of

perfect measurements will not be applicable for robustness analysis and gain tuning, but they are valid for a preliminary evaluation of the controller concept.

The results of one exemplary simulation are presented in Figures 10 and 11. Starting at a bank angle of approx. $\mu = 133°$ and an angle of attack of $-12°$, the vehicle follows the commanded angle of attack profile while maintaining the bank angle. About $t = 28\,\mathrm{s}$ into the simulation, a roll maneuver is commanded where the vehicle changes from belly-up to belly-down configuration by rolling around the velocity vector by 180° to $\mu = 47°$ and simultaneously changing the angle of attack from $-20°$ to 5°. It can be seen in Figures 10 and 11 that the controller manages to track the desired profiles very closely. The maximum resulting deviation in sideslip angle is as low as approx. 0.2°, while the deviations from the bank angle and angle of attack profiles are negligible, implying that the transformation from the commanded angles (and derivatives) to accelerations and the model inversion module are both valid.

5. Guidance Strategy

The independent variable of the guidance logic is the specific energy

$$e = \frac{v^2}{2} - \left(\frac{gm}{r_p + h} - \frac{gm}{r_p} \right) \tag{1}$$

where g is the gravitational constant, m is the planet mass, r_p is the planet radius and v is the velocity. The guidance task is to determine the control functions

$$[\mu_{\text{com}}(e), \alpha_{\text{com}}(e), \beta_{\text{com}}(e)]^T, \quad e \in [e_0, e_f] \tag{2}$$

to steer the vehicle from the current state $x(e_0)$ to the desired terminal state $x_{\text{tar}}(e_f)$. The terminal state is fixed in longitude and latitude and bounded below in altitude, the other components are free. The guidance problem shall be solved for an envelope of off-nominal conditions, mainly arising from the dispersion of the initial state due to the launch vehicle delivery inaccuracy and environmental uncertainties such as wind, variations of atmospheric density and other effects that alter the aerodynamic forces, i. e., perturbed lift and drag coefficients.

The trim conditions of the vehicle are precomputed and stored on-board as angle of attack vs. Mach profile $\alpha_{\text{ref}}(M(v,h))$. The angle of attack profile remains unchanged and the sideslip angle is zero:

$$\alpha_{\text{com}}(e(v,h)) = \alpha_{\text{ref}}(M(v,h)) \tag{3}$$

$$\beta_{\text{com}}(e(v,h)) = 0 \tag{4}$$

The vehicle is solely controlled by manipulating the lift vector through banking. The longitudinal dynamics are governed by the drag acceleration which can indirectly be controlled by adjusting the vertical lift component, which is the component directly acting against the gravitational force. Banking the vehicle also results in a parasitic lateral side force, which can be pointed to either side of the vehicle by reversing the sign of the bank angle. The longitudinal and lateral control are thus coupled. Usually the longitudinal control takes precedence, while the crossrange is a secondary control goal. For the currently investigated mission scenario however the nominal re-entry trajectory has a high curvature which requires to control both downrange and crossrange at the same time. To this end we employ a numeric prediction to compute the partial derivatives of the downrange and crossrange with respect to changes in the bank angle magnitude and the point at which the bank angle sign is reversed. Given a careful budgeting of the control authority and additional assumptions, this allows to compute an adjustment of the bank angle profile to drive the predicted downrange/crossrange error to zero as is detailed in the following.

The nominal control function is parametrized as piecewise constant segments of bank angle magnitudes and bank angle signs, given as function of specific energy. We consider the vertical lift-over-drag ratio

$$u = \frac{L}{D} \cos(\mu) \tag{5}$$

as the control variable, where L and D are the lift and drag forces acting on the vehicle. The guidance performs three predictions of the future trajectory in each guidance call using a Runge-Kutta integration scheme, starting at the current state of the vehicle until a predetermined terminal energy is reached. Let $\overset{*}{\mu}$ be the best currently known bank angle control function and let $\overset{*}{u}$ and $\overset{*}{e}_r$ denote the corresponding vertical lift-over-drag ratio and the corresponding energy point of the next bank reversal. Furthermore we define the following perturbed quantities:

$$\tilde{u} = \overset{*}{u} + \delta u \tag{6}$$

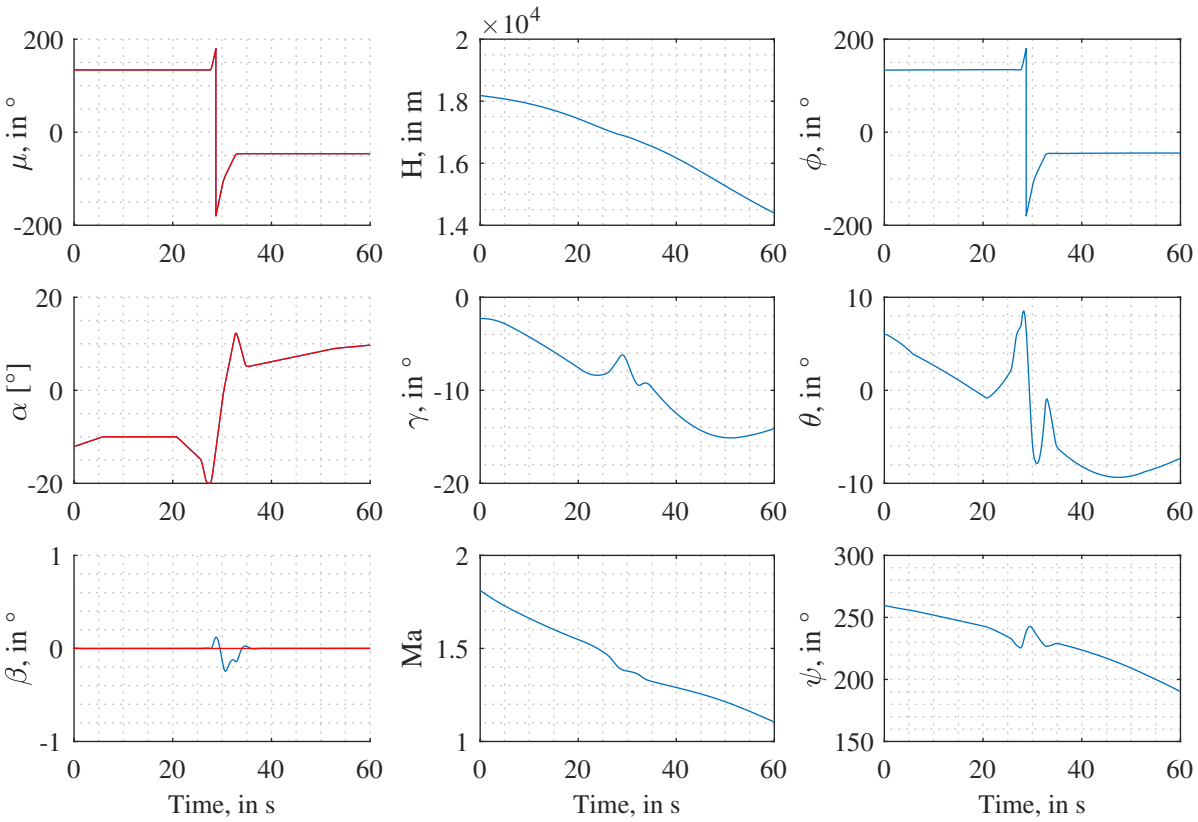

Figure 10: Results of time simulations, $T = 60\,\mathrm{s}$ (red: guidance commands; blue: simulation results).

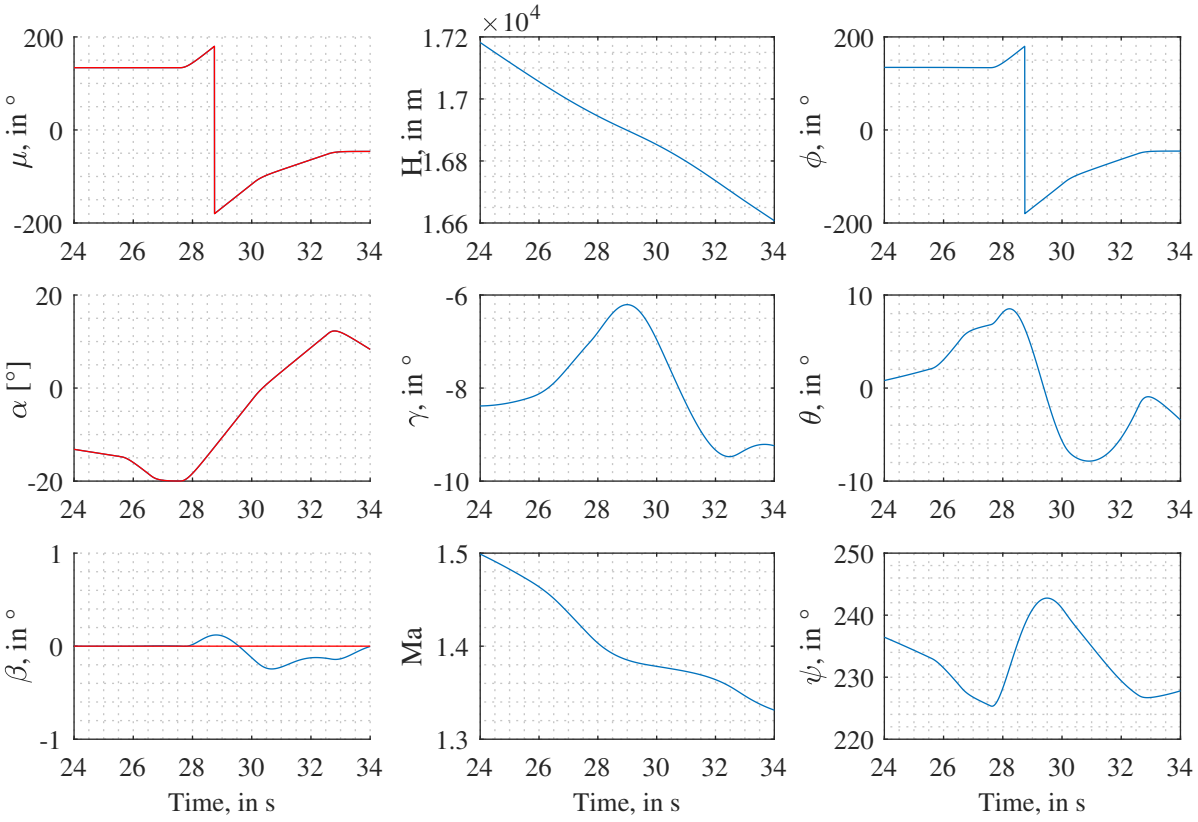

Figure 11: Results of time simulations, $T = 10\,\mathrm{s}$ centered on roll manoeuver (red: guidance commands; blue: simulation results).

$$\tilde{e}_r = \overset{*}{e}_r + \delta e \tag{7}$$

By integrating the equations of motion with the nominal and the disturbed control functions, we obtain three sets of predictions for the resulting downrange and crossrange:

$$\left[R_D\left(\overset{*}{u},\overset{*}{e}_r\right),\ R_C\left(\overset{*}{u},\overset{*}{e}_r\right)\right] \tag{8}$$

$$\left[R_D\left(\tilde{u},\overset{*}{e}_r\right),\ R_C\left(\tilde{u},\overset{*}{e}_r\right)\right] \tag{9}$$

$$\left[R_D\left(\overset{*}{u},\tilde{e}_r\right),\ R_C\left(\overset{*}{u},\tilde{e}_r\right)\right] \tag{10}$$

Using these predictions, we approximate the partial derivatives of downrange and crossrange with respect to the changes in the vertical lift and energy of next bank reversals using finite differences. The changes in the vertical lift-to-drag ratio Δu and energy of next bank reversal Δe_r required to minimize the errors in downrange ΔR_D and crossrange ΔR_C are then approximated by

$$\begin{pmatrix} \Delta u \\ \Delta e_r \end{pmatrix} = \begin{pmatrix} \frac{\partial R_D}{\partial u} & \frac{\partial R_D}{\partial e} \\ \frac{\partial R_C}{\partial u} & \frac{\partial R_C}{\partial e} \end{pmatrix}^{-1} \begin{pmatrix} \Delta R_D \\ \Delta R_C \end{pmatrix}. \tag{11}$$

Finally, the updated bank angle magnitude for the current segment is obtained as

$$|\mu_{\text{com}}| = \arccos(\overset{*}{u} + \Delta u) \tag{12}$$

and the energy point of the next bank reversal is updated as

$$e_r = \overset{*}{e}_r + \Delta e_r. \tag{13}$$

The guidance function is implemented in two cascaded loops. The predictor-corrector logic is executed in one function at a low rate, while the computed bank angle profile is evaluated at the current energy by a separate function running at a higher rate.

6. Navigation Performance Assessment

The navigation performance attainable by the HNS (described in Section 3.2) can be assessed through covariance analysis, in which the Parametric Cramér-Rao Bound (PCRB) can be used to provide a floor for the achievable filter state covariance (see, e. g., [22]). This covariance measure is initialized and propagated along the nominal mission trajectory. At appropriate epochs it is updated with statistical models of the measurements, emulating the sensor fusion algorithm within the HNS. A previous ReFEx navigation performance assessment of this kind has been published in [7]. The current analysis uses the most current sensor set and an up-to-date mission trajectory which, as described in Section 4, includes a bank-angle reversal (belly-up to belly-down) maneuver during the descent. In addition, it uses a higher fidelity model of the Sun sensors, accounting for their configuration within the vehicle and their FoV.

6.1 Trajectory

The altitude, velocity, linear acceleration and angular rate profiles of the trajectory followed are shown in Figure 12, where the time origin is the lift-off instant. The mission is split into two phases: a passively stabilized ascent and a controlled descent. During the ascent, the vehicle spins up to 900 °/s for about 80 s, being propelled by two engine burns (one per rocket stage), as is visible in Figure 12; during the descent, the atmospheric reentry decelerates the vehicle. The mentioned bank-angle reversal maneuver is performed during this phase (at around $T = 400$ s).

6.2 Sun Sensors

As above mentioned, Sun sensor mounting orientation is accounted for in this performance assessment. The used configuration can be seen in Figure 13. The sensors are placed symmetrically around the longitudinal axis each 90° apart, guaranteeing full coverage around the aforementioned axis, given their 120° FoV.

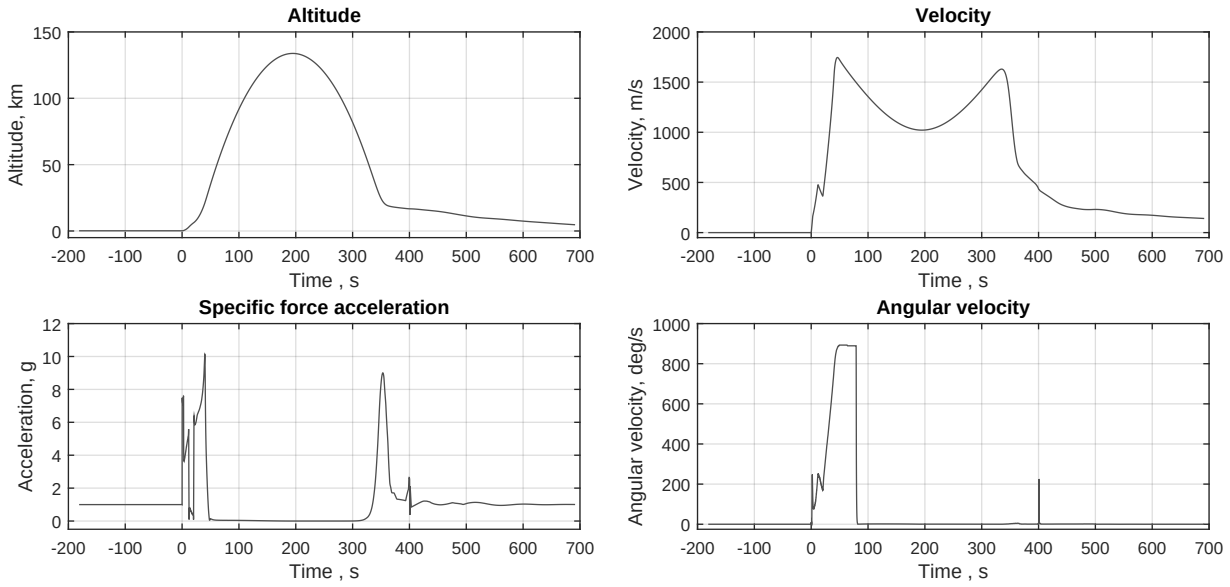

Figure 12: Altitude, total velocity, total specific-force (non-gravitational) acceleration, and angular rate profiles; lift-off at $T = 0\,\mathrm{s}$.

For the Sun sensor to work, the following conditions need to be met:

- Sun is in the FoV;
- The rotational rate is lower than 10 °/s (assumed value at which the sensor performance drop is still acceptable; however, larger than the 2 °/s used in [7]);
- Altitude is higher than 40 km (i. e., the atmospheric glow of the sky above the sensor is low enough);
- Earth is not the unit's FoV.

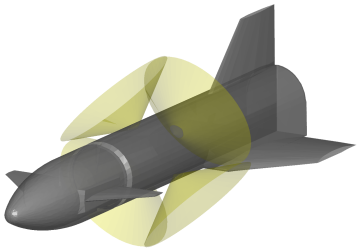

Figure 13: Current Sun sensor configuration.

Due to the large FoV of the sensors used and the proximity to Earth, it is likely that the planet is within the sunlit unit's FoV, corrupting its measurements. Also, the high spinning rate during the ascent renders the sensors unusable during this phase. Combining all the conditions above and computing accurate Sun direction at the flight location (e. g., using SPICE [23]), it is possible to estimate the measurement availability at different times. For example, in December at noon, when the Sun is at its highest point in Australia, the overall Sun sensor availability window in flight is around 100 s, as seen in Figure 14 (above). Conversely, this window is much lower in June, when the Sun is closer to the horizon, making the sensors more likely to have both Sun and Earth in their FoV simultaneously. Figure 14 (below) shows that under these circumstances, the availability window is reduced around $\sim 40\,\%$ at noon. This shows that the time of the day and of the year greatly influences the availability of Sun sensor measurements and, thus, the performance of the navigation system. The effect of these measurements (and their absence) on the HNS performance is discussed in the following point, where the best case scenario (noon in December) is compared to the total absence of these meaurements. This provides two extreme cases, which include other possible scenarios (e. g., launch in June).

6.3 Covariance Results

The results of the filter covariance analysis are displayed in Figure 15 for the HNS with and without Sun sensor aiding, with plots showing position, velocity, and attitude (2-norm) estimation errors (1σ). The initial condition (1σ) is 10 m (all Earth-Centered Earth-Fixed (ECEF) axes), 0.01 m/s (static vehicle in all ECEF directions), and 1° (all body axes). The structure of the IMU filter model used is identical to that in [7] and includes gyroscope and accelerometer bias (turn-on and drift), scale-factor (turn-on and drift), angular/velocity random walk, misalignment and G-sensitivity (gyroscope only). GPS position and velocity information updates the filter state covariance, emulating the raw GPS measurement

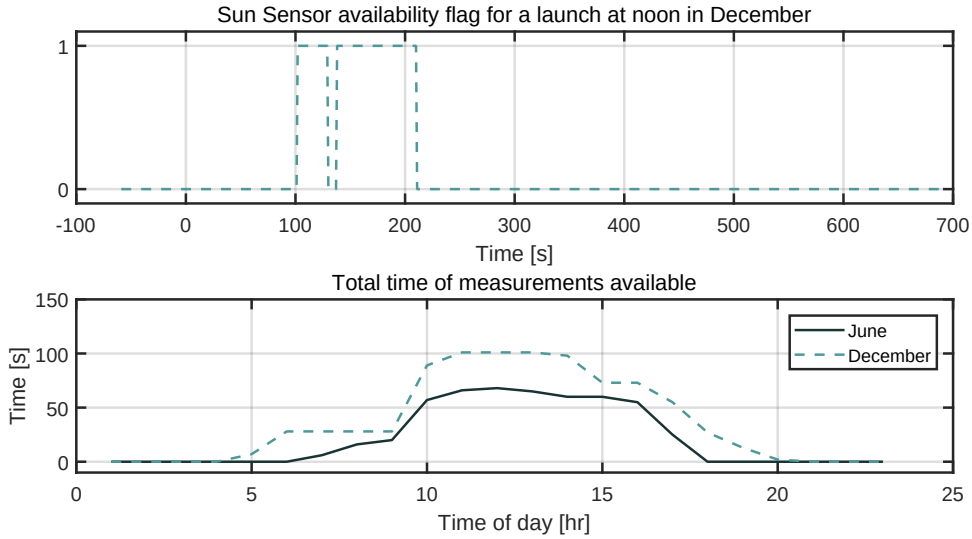

Figure 14: Sun sensor availability at noon in December (above) and time of availability with respect to month and time of the day (below).

inputs in the actual implementation of the HNS. The Sun sensor model includes the field-of-view amplitude and measurement noise. An alignment period of 180 s on the launch pad is simulated through the use of static updates (null velocity and null rate, both with respect to ECEF). As had been observed in [7], the position estimation accuracy is driven mainly by the GNSS signal quality, i. e., 8 – 10 m (1σ) during flight. Velocity and attitude errors, on the other hand, have a higher dependence on the IMU error model, with the latter being very sensitive to gyroscope performance. Velocity estimation is worse during engine burns and reentry deceleration phase (cf. Figure 12) reaching around 0.5 m/s (1σ); in contrast, steady-state accuracy lies below 0.3 m/s (1σ). As expected, and as also seen in [7], when available (cf. Figure 14), the Sun sensors considerably improve attitude estimation (from about 0.8° to about 0.3° [1σ], within $T \in [102,\ 210]$ s). Velocity and position see only a negligible benefit. At lower altitudes in the descent, when the Sun sensors no longer operate, the improvement in attitude estimation is gradually lost as the error in this state slowly tends to that of the HNS without Sun sensors.

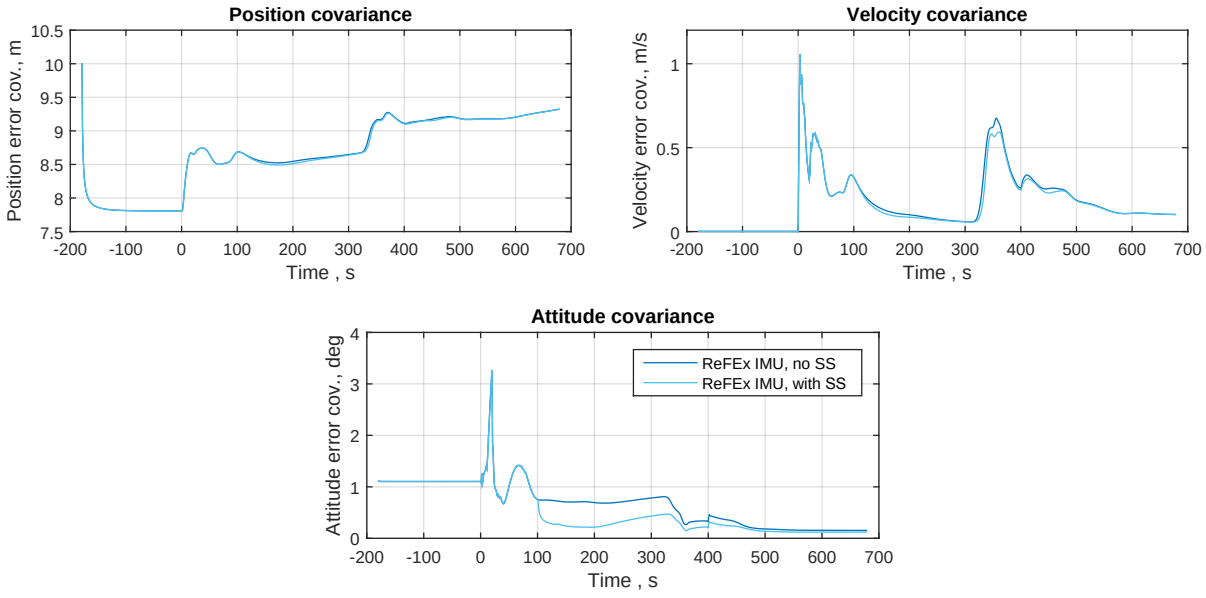

Figure 15: Kinematic state estimation error covariance (1σ) for the HNS with or without Sun sensors.

7. Conclusions and Outlook

The preliminary design of the GNC system for ReFEx has been presented. Further work to be performed is a 6-DoF closed-loop simulation of the entire GNC chain in order to validate the design of the several subsystems presented here. On the flight controller side, this will include tuning of inner loop gains and extensive robustness analysis, followed by the integration with the outer guidance loops. Re-tuning gains might be necessary to optimize the interaction between the inner and the outer loops. The future guidance design, on the other hand, requires analysis and improvement of robustness by adjusting both the predictor-corrector and evaluation functions. The presented navigation performance assessment through covariance analysis consolidates the current architecture of the HNS. Filter algorithm implementation and model-in-the-loop testing, including closing the loop with guidance and flight control functions, constitute the following steps. Furthermore, the Sun sensor availability analysis shows the effect on HNS performance. Since the sensors are important for canceling errors gained through the ascent phase, their availability time could be maximized with selection of the time of the day, another configuration and/or a controlled rolled maneuver in the phases where active guidance is not present. This will be taken into account for refining the the design.

Acknowledgements

The work described in this paper has been funded internally by the German Aerospace Center (DLR), Program Directorate Space Research and Technology, as part of the ongoing project *Reusability Flight Experiment (ReFEx)*. The authors gratefully acknowledge the joint team work and the valuable discussions with the members of the ReFEx project team and other colleagues across all DLR sites. We especially thank our colleagues

- from the Department of Safety Critical Systems & Systems Engineering of the DLR Institute of Flight Systems in Braunschweig for the development of the aerodynamic actuators,
- from the Department of Transport and Propulsion Systems of the DLR Institute of Space Systems in Bremen for the development of the Reaction Control System (RCS),
- from the Department of Spacecraft of the DLR Institute of Aerodynamics and Flow Technology in Braunschweig for the close collaboration concerning vehicle aerodynamics [24], flight controllability and stability, and
- from the Department of Supersonic and Hypersonic Technology of the same Institute with its site in Cologne for providing data from the Flush Air Data System (FADS) as part of the scientific instrumentation [25] of the vehicle for navigation purposes.

Abbreviations

API	Application Programming Interface
C/A	Coarse Acquisition
CALLISTO	Cooperative Action Leading to Launcher Innovation for Stage Tossback Operation
CAN	Controller Area Network
CNES	Centre National d'Etudes Spatiales *French Space Agency*
COTS	Commercial Off-the-Shelf
CPU	Central Processing Unit
DC/DC	Direct Current-to-Direct Current
DLR	German Aerospace Center *German: Deutsches Zentrum für Luft- und Raumfahrt e. V.*
DoF	Degrees of Freedom
EBX	Electronics Box
ECEF	Earth-Centered Earth-Fixed
EGSE	Electrical Ground Support Equipment
EMI	Electromagnetic Interference
Eu:CROPIS	Euglena and Combined Regenerative Organic-Food Production in Space
EVEREST	Evolved European Reusable Space Transport
FADS	Flush Air Data System
FDIR	Failure Detection, Isolation, and Recovery
FEE	Front-End Electronics
FOS	Fiber-Optical Sensors
FoV	Field of View
FPGA	Field-Programmable Gate Array
G&C	Guidance and Control
GCC	Guidance & Control Computer
GNC	Guidance, Navigation and Control
GNSS	Global Navigation Satellite System
GPIO	General-Purpose Input/Output
GPS	Global Positioning System
GSOC	German Space Operations Center
HiL	Hardware-in-the-Loop
HNS	Hybrid Navigation System
IMU	Inertial Measurement Unit
ISA	International Standard Atmosphere
JAXA	Japan Aerospace Exploration Agency *Japanese:* 宇宙航空研究開発機構
LEO	Low-Earth Orbit
LFBB	Liquid Fly-Back Booster
LNA	Low-Noise Amplifier

MVM	Mission Vehicle Management
OBC	On-Board Computer
OBCDH	On-Board Computing and Data Handling
OR	O-Ring
OUTPOST	Open modUlar sofTware PlatfOrm for SpacecrafT
PCI	Peripheral Component Interconnect
PCIe	Peripheral Component Interconnect Express
PCRB	Parametric Cramér-Rao Bound
PDU	Power Distribution Unit
PDU-C	PDU Controller
PDU-M	PDU Monitor
PPS	Pulse Per Second
RAAF	Royal Australian Air Force
RCS	Reaction Control System
ReFEx	Reusability Flight Experiment
RLV	Reusable Launch Vehicle
RTEMS	Real-Time Executive for Multiprocessor Systems
S/S	Subsystem
SHEFEX II	SHarp Edge Flight EXperiment II
SHEFEX III	SHarp Edge Flight EXperiment III
SMP	Symmetric Multiprocessing
TM	Telemetry
TM/TC	Telemetry and Telecommand
VTVL	Vertical Takeoff, Vertical Landing
WGS84	World Geodetic System 1984

References

[1] Martin Sippel, Chiara Manfletti, and Holger Burkhardt. Long-term/strategic scenario for reusable booster stages. *Acta Astronautica*, 58(4):209 – 221, 2006.

[2] François Deneu. *Selection and Design Process of TSTO Configurations*.

[3] Peter Rickmers and Waldemar Bauer. ReFEx: Reusability Flight Experiment – A Project Overview. In *8th European Conference for Aeronautics and Space Sciences (EUCASS), Conference on "Reusable Systems for Space Access". July 1–4, 2019, Madrid, Spain*. EUCASS association, 2019.

[4] Oliver Montenbruck, Eberhard Gill, and Markus Markgraf. Phoenix-XNS-a miniature real-time navigation system for LEO satellites. In *3rd ESA Workshop on Satellite Navigation User Equipment Technologies, NAVITEC*, pages 11–13, 2006.

[5] Markus Markgraf and Oliver Montenbruck. Phoenix-HD—a miniature GPS tracking system for scientific and commercial rocket launches. In *6th International Symposium on Launcher Technologies*, 2005.

[6] Sigtec Navigation Pty Ltd. *"MG5000 Series User Guide"; MG5-200-GUIDS-User Guide*, August 2003. Issue B-T08.

[7] M. Sagliano, G. F. Trigo, and R. Schwarz. Preliminary Guidance and Navigation Design for the Upcoming DLR Reusability Flight Experiment (ReFEx). In *69th International Astronautical Congress*, Bremen, Germany, 2018.

[8] Lars Johannsen. Erarbeitung eines Konzeptes zur aktiven Steuerung einer hochzuverlässigen Leistungsversorgungseinheit für ein hybrides Navigationssystem. Bachelor's, Hochschule Bremen, July 2015.

[9] Norbert Kwiatkowski. Entwicklung eines Referenzdesigns einer hochverfügbaren Leistungsversorgungseinheit für das Shefex III- Navigationssystem. Bachelor's, Hochschule Wilhelmshaven, January 2014.

[10] Norbert Kwiatkowski. Entwicklung von Test- und Verifikationsprozeduren für eine hochverfügbare Leistungsversorgungseinheit auf Basis einer Fehlermöglichkeits- und -einflussanalyse. Master's thesis, Hochschule Wilhelmshaven, December 2015.

[11] Samy Ayoub. Development of a Power Distribution Unit Controller for the SHEFEX III Navigation System. Master's thesis, Cologne University of Applied Sciences, July 2015.

[12] Martin Reigenborn. Development and Verification of a Power Distribution Unit Controller Software for a Hybrid Navigation System. Master's thesis, Technische Universität Berlin, October 2018.

[13] René Schwarz and Stephan Theil. A Fault-Tolerant On-Board Computing and Data Handling Architecture Incorporating a Concept for Failure Detection, Isolation, and Recovery for the SHEFEX III Navigation System. In *Proceedings of the 13th International Conference on Space Operations (SpaceOps), May 5–9, 2014, Pasadena, California*. American Institute of Aeronautics and Astronautics (AIAA), May 8, 2014. AIAA Paper No. 2014-1874.

[14] Real-Time Executive for Multiprocessor Systems. http://www.rtems.org. Accessed: 2019-06-11.

[15] Alexander Krutwig AK and Sebastian Huber SH. RTEMS SMP Status Report. 2015.

[16] OUTPOST - Open modUlar sofTware PlatfOrm for SpacecrafT. http://github.com/DLR-RY/outpost-core. Accessed: 2019-06-11.

[17] Zain A. H. Hammadeh, Tobias Franz, Olaf Maibaum, Andreas Gerndt, and Daniel Lüdtke. Event-Driven Multithreading Execution Platform for Real-Time On-Board Software Systems. In *Operating Systems Platforms for Embedded Real-Time applications (OSPERT)*, July 2019. to appear.

[18] Olaf Maibaum and Ansgar Heidecker. Software Evolution from TET-1 to Eu: CROPIS. In *10th IAA International Symposium on Small Satellites for Earth Observation*, 2015.

[19] Clemens Merrem, Viola Wartemann, and Thino Eggers. Preliminary Aerodynamic Design of a Reusable Booster Flight Ex-

periment. In *International Conference on High-Speed Vehicle Science Technology (HiSST). 26–29 November 2018, Moscow, Russia*. CEAS, 2018.

[20] Bernard Etkin and Lloyd Duff Reid. *Dynamics of Flight: Stability and Control*. John Wiley & Sons, Inc., third edition, 1996.

[21] Sven Stappert, Peter Rickmers, Waldemar Bauer, and Martin Sippel. Mission Analysis and Preliminary Re-entry Trajectory Design of the DLR Reusability Flight Experiment ReFEx. In *8th European Conference for Aeronautics and Space Sciences (EUCASS), Conference on "Reusable Systems for Space Access". July 1–4, 2019, Madrid, Spain*. EUCASS association, 2019.

[22] Niclas Bergman. *Recursive Bayesian Estimation: Navigation and Tracking Applications*. PhD thesis, Linköping University, Sweden, 1999.

[23] NASA. The SPICE Concept. https://naif.jpl.nasa.gov/naif/spiceconcept.html. Accessed: 2019-06-16.

[24] Clemens Merrem, Daniel Kiehn, Viola Wartemann, and Thino Eggers. Aerodynamic Design of a Reusable Booster Stage Flight Experiment. In *8th European Conference for Aeronautics and Space Sciences (EUCASS), Conference on "Reusable Systems for Space Access". July 1–4, 2019, Madrid, Spain*. EUCASS association, 2019.

[25] Thomas Thiele, Frank Siebe, Andreas Flock, and Ali Gülhan. Flight Instrumentation for the Reusability FlightExperimentReFEx. In *8th European Conference for Aeronautics and Space Sciences (EUCASS), Conference on "Reusable Systems for Space Access". July 1–4, 2019, Madrid, Spain*. EUCASS association, 2019.